University of Stavanger

Faculty of Science and Technology

MASTER'S THESIS

Study program/ Specialization: MSc in Environmental Technology/ Offshore Environmental Engineering	Spring semester, 2012 Open / ~~Restricted access~~
Writer: Camilla Gosvig Overgaard	…… (Writer's signature)

Faculty supervisor: Torleiv Bilstad

External supervisor(s): William A. Arnold, professor at the University of Minnesota

Title of thesis:

Adsorption of the phytoestrogens, genistein and daidzein, onto the iron oxide-hydroxide goethite.

Credits (ECTS): 30

Key words: Phytoestrogens, genistein and daidzein Goethite Adsorption isotherm Sorption edge	Pages: 35 + enclosure: 9 Stavanger, 13th of July 2012 Date/year

Abstract

Genistein and daidzein are plant-derived compounds called phytoestrogens, and they are found in high concentrations in legumes, primarily soy. Phytoestrogens function as endocrine disrupting chemicals (EDCs) in animals when assimilated in high doses. Changed secondary sex characteristics and reduced fertility have been observed in fish due to these endocrine disrupting abilities of phytoestrogens. The role of phytoestrogens as environmental contaminants is highly relevant because of the growing soy-based biofuel industry.

This thesis examines the extent to which genistein and daidzein adsorb onto goethite nanoparticles (α-FeO(OH)). The goethite simulates sediment consisting of iron particles and suspended solids in water. The aim of this thesis is to investigate the fate of genistein and daidzein when they are discharged in water bodies with ferruginous sediments, and whether they get removed from the aqueous phase or stay dissolved.

Standard batch adsorption experiments were carried out for genistein and daidzein onto goethite, and adsorption isotherms and sorption edges were made from the results. Furthermore the specific surface area (SSA_{TEM}) of the goethite nanoparticles was calculated using TEM-pictures, and the pK_a values for goethite were found and calculated from standard potentiometric titrations.

SSA_{TEM} of the goethite nanoparticles was found to be 248 $m^2/g \pm 90$ m^2/g, while the specific surface area determined through BET-analysis, SSA_{BET}, was measured to 118.5 $m^2/g \pm 2.6$ m^2/g. Furthermore the pK_a values for goethite were calculated at pH 6.73 and 10.34, and the pH of point zero charge, pH_{pzc}, was found at 8.3.

The isotherm and sorption edge results showed that adsorption of genistein and daidzein onto goethite is pH-dependent and also independent of the adsorbate concentrations at these relatively low environmental relevant concentrations. For genistein, the adsorption decreased constantly with increasing pH. The highest adsorption capacity was at pH 4.7 with a K_D at 0.00431 L/m^2 and a percent mass adsorbed at 84 %. At pH higher than 7.4, the adsorption capacity started decreasing rapidly, to a minimum of 17 % mass adsorbed and a K_D of 0.000168 L/m^2 at pH 9.7. Daidzein was only removed to a limited degree and had an adsorption maxima at pH 7.4, with 27 % mass adsorbed and a K_D at 0.000307 L/m^2. K_D and the percent mass adsorbed were slightly lower from pH 4.7 to 7.4. The minimum adsorption capacity for daidzein was found at pH 9.7, with a K_D of 4.66691E-06 L/m^2 and only 1 % mass adsorbed.

Hydrophobic interactions or surface complexations were suggested as the adsorption mechanisms at low pH for both genistein and daidzein. Electrostatic repulsion was proposed to be the reason for the drop in adsorption capacity at higher pH, when the compounds get deprotonated.

Applying the results to determine the fate of phytoestrogens in the environment, it is clear that genistein will be removed by adsorption to a greater extent than daidzein, when released to ferruginous natural waters. The removal of the phytoestrogens from the water phase through adsorption is significantly higher at low pH compared to high pH values, and thus the adsorption mechanism is more relevant for low pH waters.

Acknowledgement

First of all I wish to thank my faculty advisor Professor Torleiv Bilstad, for his guidance and for giving me the opportunity to go to the States. It has been an amazing journey! I would also like to thank my advisor at the University of Minnesota in Minneapolis, Professor William A. Arnold, for giving me this assignment and taking me in as a student. He has been a great technical advisor and has been most helpful. I am grateful to PhD-student Megan M. Kelly, who has been happy to help in the laboratory and has answered a lot of questions during the last six months. Also, I wish to thank Amanda Stemig for synthesizing and characterizing the goethite particles. I am grateful to Nate Fleischhacker, Greg Lefevre and David Tan for laboratory assistance and for creating a good environment in the laboratory. I am most thankful to the University of Minnesota for letting me use their facilities during the three month stay.

I also wish to acknowledge all the nice people that made our stay as incredible as it was. Especially the Palmer Family for taking us in, serving us great food, taking care of us, showing us around and giving us insight to the American culture and traditions.

I wish to give a special thanks to my dear friend and co-traveler, Cecilie Brekke for choosing to go to Minneapolis together with me. It would not have been the same without her!

At last, I want to thank my beloved Helge Rørvik, who has encouraged me to follow my dreams and let me travel away for three months. I thank him for helping and supporting me for the last five years and for talking sense into me, when I thought about giving up on an education I thought was too difficult for me. I am eternally thankful for that.

I thank you all for your help, kindness and patience.

Table of Content

List of Figures

List of tables

Abbreviations

DAD	Diode-Array Detection
EDC	Endocrine Disrupting Chemical
ER	Estrogen Receptors
HPLC	High-Performance Liquid Chromatography
pH_{pzc}	pH of Point Zero Charge
SA	Surface Area
SSA	Specific Surface Area
SSA_{BET}	Specific Surface Area measured using BET analysis
SSA_{TEM}	Specific Surface Area calculated from TEM pictures
TEM	Transmission Electron Microscope
KD	Adsorption

1. Introduction

During the 1940s in Australia it was observed that sheep grazing on clover experienced temporary or permanent infertility. At that time knowledge about the effects of phytoestrogens was uncharted. Today, however, research shows that clover has a high content of phytoestrogens (Kiparissis et al., 2003).

Phytoestrogens are plant-derived compounds that functions as endocrine disrupters in animals when assimilated in high doses. The study of phytoestrogens as potential environmental contaminants is a relatively new area of interest. Cases of reduced fertility and changed secondary sex characteristics in animals due to exposure to phytoestrogens have gradually been documented. Fish and other aquatic animals are exposed to phytoestrogens, not only through their diet, but also to dissolved phytoestrogens in the aqueous phase (Clotfelter and Rodriguez, 2006).

This thesis focuses on the two phytoestrogens, genistein and daidzein, and investigates how they adsorb onto the iron hydroxide goethite (α-FeO(OH)). The goethite simulates sediment consisting of iron particles and suspended solids in water. The aim of this thesis is to investigate the fate of genistein and daidzein when they are discharged in water bodies with ferruginous sediments, whether they get removed from the aqueous phase or stay dissolved. This is an important factor when evaluating the environmental impact of released phytoestrogens.

Isotherm and sorption edge experiments were carried out to investigate the mechanism of adsorption and the amount of phytoestrogens adsorbed onto goethite. Experiments for this thesis were executed in Minneapolis at the University of Minnesota from January 16th to April 12th. The experiments are part of a bigger project regarding adsorption of phytoestrogens to different kinds of sediment particles, carried out by PhD student Megan M. Kelly under the supervision of Professor William A. Arnold. Megan Kelly is examining the adsorption of genistein and daidzein to different kinds of clay; i.e. kaolinite, Na-montmorillonite, Ca-montmorillorite, natural sediment from Minnesota River (Mankato, MN) and from Okabena Creek (Brewster, MN). Ms. Kelly's results will be published with the results of this thesis late 2012 or early 2013.

2. Background

2.1 Phytoestrogens

Phytoestrogens are xenoestrogens synthesized by plants, and they are classified as endocrine disrupters. There are especially high concentrations of these in the family of legumes, such as soybean and red clover. With a content of 10^7 µg/kg, soy contains the highest phytoestrogens levels of any plant (Lundgren and Novak, 2009).

Phytoestrogens are natural phenolic compounds and are divided into three groups: isoflavones, coumestans and lignans. This thesis focuses on the two isoflavones genistein and daidzein (Figure 2.1a and 2.1b). The acid dissociation constants (pK_a) of genistein are 7.2, 10.0 and 13.1 (Zielonka, 2003, Kelly and Arnold, 2012) and the different states of protonation are named H_3GEN, H_2GEN^-, $HGEN^{2-}$ and GEN^{3-}. For daidzein the states of protanation are H_2DDZ, $HDDZ^-$ and DDZ^{2-} according to the following pK_a values of 7.5 and 9.7 (Liang et al., 2008). Genistein and daidzein are photosensitive and have half-lives estimated at 35.5 and 0.34 hours, respectively. While genistein is degraded mainly through indirect photolysis (via reactions with triplet-state natural organic matter), daidzein is degraded through direct photolysis and singlet oxygenation (Kelly and Arnold, 2012).

Phytoestrogens are structurally very similar to the animal estrogen 17-β-estradiol (Figure 2.1c) and are therefore able to function as estrogens in animals when assimilated (Lundgren and Novak, 2009, Ardia and Clotfelter, 2006, Clotfelter and Rodriguez, 2006). The structural similarity is seen in Figure 2-1.

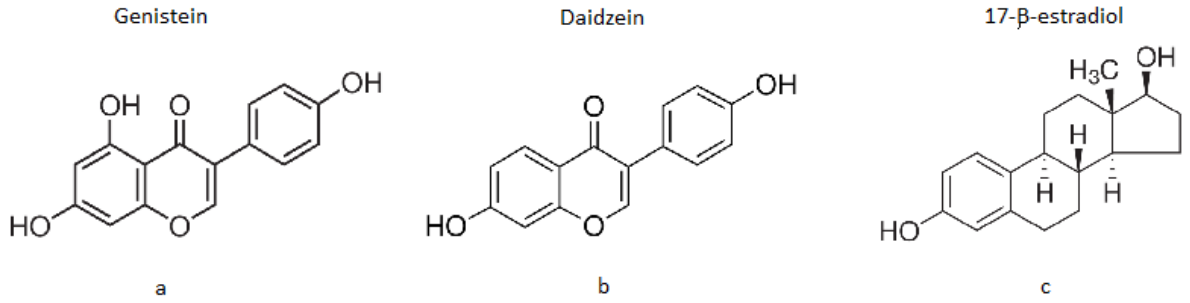

Figure 2-1: Structures of genistein (a), daidzein (b) and 17-β-estradiol (c)(Sigma-Aldrich).

The ability to act like estrogens in animals makes phytoestrogens endocrine disrupting chemicals (EDCs), but they function as EDCs in different ways. Phytoestrogens mainly function as agonists and act estrogenic by binding to estrogen receptors (ER). Phytoestrogens bind to ER with high affinity because of their similarities to estrogen (Latonnelle et al., 2002). The most important similarities in the structure include a low molecular weight, the phenolic ring that is essential for binding to an ER, the distance between the two hydroxyl groups and the similar shape of the binding site – the bay region (Turner et al., 2007). Phytoestrogens may also act as antagonists by blocking the estrogen

receptors, or binding itself to the target molecule of the receptor and inactivating it (Lund et al., 2004).

Phytoestrogens are mainly discharged into surface waters from effluents of a diverse range of plant-processing industries. Due to the high content of phytoestrogens in soy, the soy industry is of particular interest. Of concern is not only the industry producing soy-based food, but also the biofuel industry based on soy. The biofuel industry is of significant importance due to the rapid increase in biofuel production (Lundgren and Novak, 2009). Another source of phytoestrogens is the pulp and paper mill industry.

A threshold of total phytoestrogens ≤ 1 µg/L is suggested to avoid impact on the environment (Thorpe et al., 2003, Latonnelle et al., 2002). Several studies have, however, shown much higher concentrations of different phytoestrogens at different locations. The study "*Quantification of Phytoestrogens in Industrial Waste Streams*" by Mark S. Lundgren and Paige J. Novak (2009) documented concentrations up to 151 µg/L and 108 µg/L of genistein and daidzein, respectively, in the waste streams of soy processing industries. From the biodiesel industry levels of genistein were measured up to 10.3 µg/L and 11.9 µg/L for daidzein. In non-soy food processing industries, such as dairy and meat, maximum concentrations of genistein and daidzein were lower at 27.5 µg/L and 12.4 µg/L, respectively. An interesting thing to notice in the study by Lundgren and Novak (2009) are the high total phytoestrogen concentrations in the inlet of waste water treatment plants and the relatively low concentrations in the effluents. This suggests that most of the phytoestrogens are degraded during treatment, but the mechanisms at which they are degraded are yet to be appointed. Another study showed that pulp and paper mills also are of concern with a genistein concentration of 10.5 µg/L in treated effluents (Kiparissis et al., 2001). All the concentrations above have been found in effluents from different kinds of industries. Genistein and daidzein, however, have also been found in surface waters around the world. In Osaka River in Japan, the genistein concentration was reported at 143.4 µg/L, whereas daidzein was measured to 42.9 µg/L (Kawanishi et al., 2004). The sampling points in the Osaka river lie in urban areas close to food and pulp factories. In Iowa, with high agricultural activity, genistein was found at a concentration of 8 ng/L in streams, together with daidzein at 41 ng/L (Kolpin et al., 2010).

Phytoestrogens are important components in human and animal diets. Terrestrial animals are exposed to phytoestrogens primarily through digesting legumes and aquatic animals are exposed both through their diet and the water phase (Clotfelter and Rodriguez, 2006, Ardia and Clotfelter, 2006). Farmed fish are especially exposed though their diet, due to the high levels of soya and alfalfa in the vegetable components of fish fodder (Kiparissis et al., 2003).

The effects of phytoestrogens are many and serious due to their effect as EDCs. They have been found to induce behavioral changes in male fish, such as less aggressive behavior towards intruders, less probability of constructing nests in the presence of females and smaller size of the nests

(Clotfelter and Rodriguez, 2006). Phytoestrogens have also been suggested to be immunosuppressive due to weaker inflammatory responses than normal under exposure of phytoestrogens (Ardia and Clotfelter, 2006). Changes to more feminized secondary sex characteristics have been observed in male Japanese Medakas as a result of exposure to high concentrations of genistein. Another effect in the male fish was a lower density of mature sperm cells. Female Japanese Medaka exposed to genistein showed delayed maturation of oocytes in the ovaries and altered ovaries. Masculinization of the secondary sex characteristics was also documented as male-like appearances of dorsal and anal fins was observed (Kiparissis et al., 2003). Due to their fertility reducing mechanism it has been suggested that phytoestrogens are a defense mechanism for plants to control the herbivore population feeding on them (Wynne-Edwards, 2001).

2.2 Goethite

Goethite is an iron oxide-hydroxide and its chemical structure is α-FeO(OH). The color of goethite is orange brownish. Goethite is a natural mineral and can be found as iron ore along with other iron oxides such as hematite (α-Fe_2O_3) and magnetite (Fe_3O_4). Nanoparticles of goethite are found naturally, and they form from weathering of iron and iron-rich minerals. Because iron is the most abundant transition metal found on Earth, goethite is found most places. In addition, goethite is thermodynamically very stable compared to other naturally formed iron oxides, which makes the tendency for accumulation of goethite larger. Goethite nanoparticles accumulate especially in soils and sediments. Because of their small size, goethite nanoparticles are also found in all natural water systems such as groundwater aquifers, rivers, lakes and oceans (Hochella Jr et al., 2007, Tribe and Baja, 2004).

Goethite nanoparticles are needle-shaped with large reactive surfaces. The functional group in goethite - the hydroxyl group - at the surface of the particles can bind strongly to both organic and inorganic ligands. This gives them a natural role as carriers of compounds and elements in water streams (Hochella Jr et al., 2007, Tribe and Baja, 2004). Goethite particles vary in size, but with reference to adsorption properties, the area to volume ratio is of interest. This ratio is also called the specific surface area (SSA). The smaller the particles get, the bigger the SSA gets, which also gives more surface functional groups per area. Calculation of the specific surface area is described in Section 3.2.1, Materials and Methods. Smaller goethite particles are often more reactive than bigger particles of the same material, due to a bigger specific surface area. Due to the fact that goethite and other iron oxide nanoparticles are everywhere in the environment, they constitute an important amount of the potentially reactive surface area present in nature (Hochella Jr et al., 2007).

The surface charge on the goethite is important because it will affect the rate or extent of adsorption. The goethite surface charge depends on the amount of ionization of the functional group -OH, which makes the surface charge dependent on pH according to the protonation sequence in Equation 2.1 (Brezonik and Arnold, 2011).

(2.1) $$\equiv \mathrm{Fe-OH_2^+} \overset{pK_{a1}}{\leftrightarrow} \equiv \mathrm{Fe-OH} + \mathrm{H^+} \overset{pK_{a2}}{\leftrightarrow} \equiv \mathrm{Fe-O^-} + \mathrm{H^+}$$

The symbol ≡ indicates that the rest of the coordination sites on the iron atom are attached to a solid surface. The uptake and release of protons are described by the acidity constants K_{a1} and K_{a2} shown in Equation 2.2 and 2.3 (Stumm and Morgan, 1995).

(2.2) $$\mathrm{K_{a1}} = \frac{\{\equiv \mathrm{Fe-OH}\}[\mathrm{H^+}]}{\{\equiv \mathrm{Fe-OH_2^+}\}}$$

(2.3) $$\mathrm{K_{a2}} = \frac{\{\equiv \mathrm{Fe-O^-}\}[\mathrm{H^+}]}{\{\equiv \mathrm{Fe-OH}\}}$$

The bracket [ ] denotes the concentration in moles/L (M), while { } implies that the concentrations of surface species is in moles/kg of adsorbing solid.

According to Equation 2.1, goethite particles in solution at low pH will have a net positive charge, while they will have a net negative charge at high pH. At a certain pH in between, the particles will have a net zero charge, where the number of protonated surface sites equals the number of deprotonated sites. This pH is called the pH of point zero charge (pH_{pzc}). At pH_{pzc}, the particles have lower stability and tend to collide more frequently, agglomerate and precipitate. Charged surfaces of goethite tend to repel each other at lower or higher pH, where they experience net negative or positive surfaces charges. The value of pH_{pzc} for goethite is reported at 7.8 in literature (Brezonik and Arnold, 2011). The pH_{pzc} value may vary some depending on which method is used to determine it, as well as the amount of surface functional groups for the specific goethite particles studied, measured in mol/m^2.

2.3 Adsorption

Adsorption is the attachment of molecules onto a surface. It is a mass transfer and accumulation process where molecules are transferred from the liquid to the solid phase. The molecule that gets transferred is called the adsorbate, while the solid phase it adheres to is called the adsorbent. In this thesis the adsorbent is goethite, while daidzein and genistein are adsorbates (Metcalf & Eddy et al., 2003, Brezonik and Arnold, 2011).

Sometimes the word “sorption” is used instead of adsorption. Sorption covers both adsorption and absorption and is used when there is uncertainty which process is causing removal of material from a suspension. While adsorption is the attachment onto a two-dimensional surface, absorption is the attachment into a three-dimensional structure. Desorption is the opposite mechanism of adsorption

and absorption and is the detachment of material. When the adsorption capacity of the adsorbent is reached, desorption equals adsorption and equilibrium is reached (Brezonik and Arnold, 2011, Metcalf & Eddy et al., 2003).

Adsorption is a consequence of interactions between solutes and surfaces. These interactions are many and include the following attractive or repulsive forces (Brezonik and Arnold, 2011):

- Chemical forces (covalent bonds)
- Long-range electrical (electrostatic) forces
- Dipole-dipole interactions, called orientation energy
- London-van der Waals forces (induced dipoles)
- Hydrogen bondings

The chemical forces are short-ranged but very strong, while electrostatic and London-van der Waals forces are weaker but effective over longer distances (Stumm and Morgan, 1995).

Properties of compounds that affect adsorption processes are solubility, polarity, and molecular structure of the adsorbate and adsorbent. Besides being dependent on the properties of both the adsorbate and the adsorbant, the adsorption process also depends on temperature and the concentration of the adsorbate (Metcalf & Eddy et al., 2003). Surface charges are also important for adsorption reactions. They arise in different ways, mainly from the presence of ionizable groups and isomorphic substitution. Surface charges due to presence of ionizable groups, such as –OH, are pH-dependent, (see Section 2.2). Isomorphic substitution is when the surface gets a permanent change in charge because a metal center in a molecule is substituted with a metal with lower charge (Brezonik and Arnold, 2011).

Types of adsorption include surface complexation reactions and the hydrophobic adsorption. Surface complexation reactions are reactions between ionizable surface sites and ligands. Hydrophobic adsorption happens because of the tendency of hydrophobic molecules to self-associate. Hydrophobic molecules in solution may adsorb to nonpolar surfaces in order to gain minimum contact with water (Brezonik and Arnold, 2011).

2.3.1 Adsorption Isotherms

An adsorption isotherm shows the relationship between the concentration of the adsorbate in solution and the amount of material adsorbed onto the solid at constant temperature. While temperature and pH are constant, the concentration of the adsorbate changes until equilibrium is reached (Metcalf & Eddy et al., 2003, Brezonik and Arnold, 2011). At equilibrium, when the adsorption rate equals the desorption rate, the remaining amount of adsorbate in the solution is

measured. The mass of the adsorbate that has been adsorbed can then be calculated from Equation 2.4.

(2.4) $$\text{Mol adsorbed} = (C_0 - C_w)\,V$$

C_0 is the initial concentration (mmol/L), C_w is the concentration in the solution at equilibrium (mmol/L), and V is the volume (L). The adsorption capacity C_s of the adsorbent (mmol/m^2) is further calculated from Equation 2.5.

(2.5) $$C_s = \frac{\text{Mol adsorbed}}{M_s A}$$

M_s is the mass of adsorbent in the solution (kg), and A is the specific surface area of the adsorbent (m^2/kg). C_s is plotted against C_w for a standard isotherm plot (Figueroa and Mackay, 2005). The Freundlich and Langmuir equations are often used to describe experimental adsorption data, but the data may also have a linear appearance and fit to a straight line. In the following subsection, the different equations to describe sorption isotherms will be explained.

2.3.1.1 Linear Isotherm

The linear isotherm is the simplest adsorption isotherm and is used when C_s plotted against C_w has a linear appearance. Equation 2.6 applies for linear correlation.

(2.6) $$C_s = K_D C_w$$

K_D is the adsorption coefficient (L/m^2) and is found from the experimental data as the slope of the trendline (Figueroa and Mackay, 2005, Arnold, 2012). K_D can also be expressed in L/kg using the specific surface area (m^2/kg) of the solid.

2.3.1.2 Freundlich Isotherm

This is the oldest model that is used to describe the relationships between concentrations of adsorbates in a solution and the amount that has been adsorbed. The Freundlich isotherm is expressed in Equation 2.7.

(2.7) $$X = K_F C^{1/n}$$

X is the amount of adsorbate adsorbed per mass of adsorbent (µg/g).

K_F is the Freundlich constant.

C is the concentration of adsorbate in the solution at equilibrium (M or mg/L) and is denoted as C_w in Equation 2.4 and 2.6.

n is an empirical factor.

The equation collapses to the linear isotherm when *n* = 1. The coefficients *n* and K_F are determined by plotting log C (x-axis) versus log C. The slope of the plot gives the coefficient *n*, and K_F is found at the point of interception on the y-axis. If the data fit to the model, they will form a straight line (Brezonik and Arnold, 2011, Stumm and Morgan, 1995).

2.3.1.3 Langmuir Isotherm

The Langmuir isotherm is based on the assumption that all sorption sites on the surface are identical, which means that they all bind with the same strength for one type of sorbate. Another important assumption is that no more than a monolayer of adsorbate onto the surface is possible. The Langmuir isotherm is defined according to Equation 2.8.

(2.8) $$\mathrm{X} = \frac{\mathrm{X_{max}}\, K_L \mathrm{C}}{1 + K_L \mathrm{C}}$$

X is the mass of adsorbate adsorbed per mass of adsorbent (µg/g).
X_{max} is the maximum adsorption capacity, an empirical constant.
K_L is the binding constant related to the energy of adsorption (L/µg)
C is the concentration of adsorbate in the solution after adsorption at equilibrium (M or mg/L) and is denoted as C_w in Equation 2.4 and 2.6.

The coefficients X_{max} and K_L are found by inverting both sides of Equation 2.8, yielding Equation 2.9.

(2.9) $$\frac{\mathrm{C}}{\mathrm{X}} = \frac{1}{\mathrm{X_{max}}\, K_L} + \frac{\mathrm{C}}{\mathrm{X_{max}}}$$

C (x-axis) is plotted against C/X. If the data fit to the Langmuir model, they will form a straight line. $1/X_{max}K_L$ is found from the point of interception on the y-axis and the slope of the line makes $1/X_{max}$ (Brezonik and Arnold, 2011, Stumm and Morgan, 1995).

2.3.2 Sorption Edges

Sorption edges are graphs developed to show the effect of pH on adsorption processes. As mentioned earlier, the charge of particle surfaces with ionizable groups is pH-dependent. Such surfaces have a net positive charge at low pH and will favor adsorption of anions onto them. The opposite will happen at high pH, where anions will experience electrostatic repulsion due to a net negative surface charge on the adsorbent (Brezonik and Arnold, 2011). Sorption edge experiments are very similar to isotherm experiments, however, the concentration of the adsorbate is kept

constant, while the pH is varied. C_s and C_w are calculated as in Equation 2.5. The adsorption coefficient K_D (L/m^2) can be calculated from a simple rearrangement of Equation 2.6 resulting in Equation 2.10.

(2.10) $$K_D = \frac{C_s}{C_w}$$

A graph is made with pH (x-axis) and the sorption coefficient K_D (y-axis), in which the correlation between the sorption coefficient and pH is seen (Figueroa and Mackay, 2005).

3. Materials and methods

3.1 Chemicals

Daidzein and genistein were both produced by TCI (Tokyo chemical industry; Tokyo, Japan). MOPS (3-(N-morpholino)propanesulfonic acid), sodium perchlorate and hydrochloric acid 37 % were produced by Sigma-Aldrich (St. Louis, MO). Both ammonium acetate and sodium hydroxide pellets were obtained from Mallinckrodt Inc. (Paris, KY). Methanol was bought from VWR international (West Chester, PA) and HPLC grade acetonitrile (ACN) was from J.T. Baker (Phillipsburg, NJ). Ultrapure water (18.2 MΩ·cm) was obtained from Milli-Q purification system from the company Millipore (Billerica, MA).

3.2 The Making and Characterization of Goethite Particles

The goethite particles were made by Amanda Stemig using the procedure described in (Chun et al., 2006). The goethite mineralogy was confirmed, also by Amanda Stemig, using X-ray diffraction (XRD). The machine used was a PANalytical X-Pert PRO MPD X-ray diffractometer.

The specific surface area (SSA) for the goethite was obtained by two different methods. The first method was N_2 BET analysis. BET analysis measures the average SSA of the particles using adsorption isotherms. The analysis was carried out by Nicholas Petkovich using a Quantachrome Autosorb iQ2-MP with N_2 as the adsorbate. The other method for obtaining the SSA is by measuring length and width of the particles using pictures taken with a transmission electron microscope (TEM) and then calculating the SSA from the numbers (SSA_{TEM}). Pictures of the goethite particles were taken by Amanda Stemig using a FEI Technai T12 TEM, at the Characterization Facility at the University of Minnesota. Length and width of 500 random particles were measured using the program ImageJ 1.45. One of the pictures taken with the TEM is shown in Figure 3-1 with a scale bar.

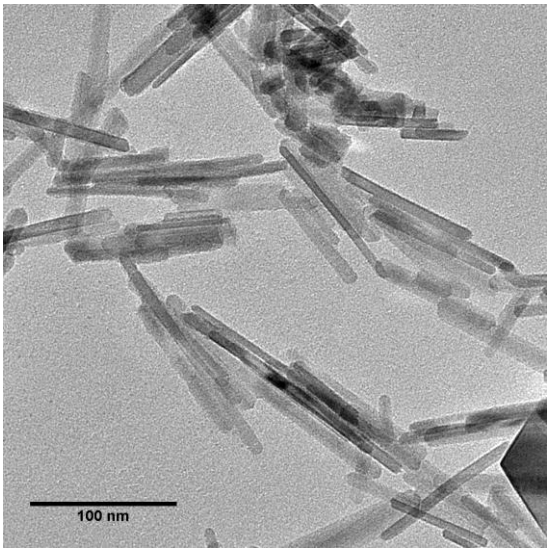

Figure 3-1: TEM picture of goethite particles

When using the SSA_{TEM} method, assumptions of the particle shape are made. SSA_{TEM} was calculated from the measured length and width (Anschutz and Penn, 2005, Stemig, 2012). The calculations are explained in the subsection "Calculations". The advantage of determining SSA using BET analysis (SSA_{BET}) is that fine surface structures are included in the SSA as well, while surface structures are ignored when calculating the SSA from pictures taken with a TEM microscope.

3.2.1 Calculations of SSA

SSA is measured in m^2/kg. The cross section of a goethite particle is rhomboidal as seen in Figure 3-2, and the angle θ is 46.7°. The density of goethite is 4.26 g/cm^3 (Anschutz and Penn, 2005).

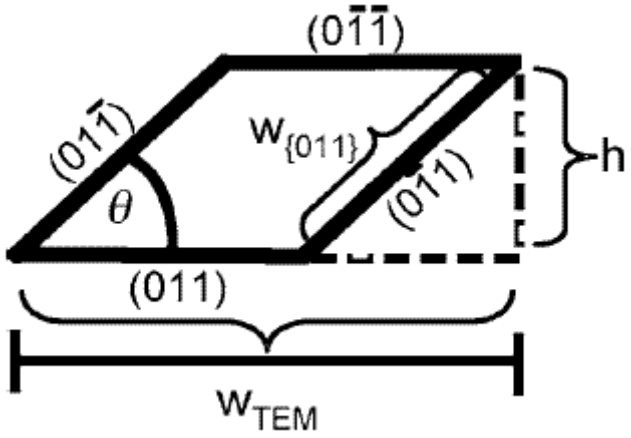

Figure 3-2: Cross section of a goethite particle (Anschutz and Penn, 2005).

θ (46.7°) was converted to 0.8151 radians using the conversion factor in Equation 3-1.

(3.1) $$\text{radians} = \frac{\theta * \pi}{180}$$

The width of the particle (w_{011}) and the height (h) in Figure 3-1 was calculated from the measured width (w_{TEM}) using Equations 3.2 and 3.3.

(3.2) $$w_{011} = \frac{w_{TEM}}{(1 + \cos(0.8151))}$$

(3.3) $$h = w_{011} * \sin(0.8151)$$

The surface area (SA) of a rhomboidal particle is calculated from the formula in Equation 3.4.

(3.4) $$SA = 4 (w_{011} * length_{TEM}) + 2 (w_{011} * h)$$

The mass of a particle can be calculated from Equation 3.5.

(3.5) $\text{Mass} = h * \text{length}_{TEM} * w_{011} * \text{density}$

Combining 3.4 and 3.5, the SSA can be calculated from Equation 3.6.

(3.6) $$SSA = \frac{SA}{Mass}$$

3.3 Instruments

The HPLC (high-pressure liquid chromatography) was a 1200 series HPLC from Agilent Technologies. The HPLC had both UV and diode-array detection (DAD). The column used in the HPLC was a Supelco Ascentis RP-amide, 15 cm x 4.0 mm, with a particle size of 5 µm. A guard column of the brand Ascentis RP-amide supelguard, 2 cm x 4.0 mm, with a particle size of 5 µm was put in front for protection of the analytical column. The mobile phase was a 10 mM ammonium acetate buffer (90 % HPLC grade acetonitrile and 10 % deionized water) with pH 5.

The pH and potential (in mV) was measured with a Fischer Scientific accumet AP62 portable pH/mV meter. The pH meter was calibrated daily before use. An Eppendorf centrifuge 5415D was used for centrifuging.

3.4 Solutions

Stock solutions were prepared in advance of the experiments as described in Table 3-1. Some were made multiple times.

Table 3-1: Stock solutions made for the experiments.

Concentration [M]	Solute	Solvent
0.001	Daidzein	Methanol
0.001	Genistein	Methanol
0.2	HCl	Water
0.05	HCl	Water
0.01	MOPS	Water
0.1	$NaClO_4$	Water
0.1	NaOH	Water
0.025	NaOH	Water

The solutions of daidzein and genistein were stored in the dark to avoid photolysis of the dissolved compounds. A 0.01 M ammonium acetate buffer for the HPLC was made from 0.7708 g ammonium acetate, 100 mL HPLC grade acetonitrile and 900 mL deionized water. The pH was adjusted by adding hydrochloric acid (HCl) to pH 5.

3.5 Standard Potentiometric Titration

A standard potentiometric titration was performed according to the procedure in Aquatic Chemistry by Stumm and Morgan (Stumm and Morgan, 1995) to find the pKa values for goethite.

0.147 g goethite was mixed with 100 mL 0.1 M $NaClO_4$ to reach a solid-to-water concentration of 1.47 g/L. The solution was acidified by adding 0.2 M HCl to a pH of 4.4. The solution was titrated with 0.1 M NaOH until pH 11.5 was reached.

To make the titration curve more detailed and precise, the experiment was repeated, but with a HCl and NaOH of ¼ the concentrations given above. In addition, the concentration of the goethite was doubled. 0.2942 g goethite was mixed with 100 ml 0.1 M $NaClO_4$ to reach a solid-to-water concentration of 2.942 g/L. 2 mL of 0.05 M HCl was added to acidify the solution down to pH 3.5 and fully protonate the goethite particles. The solution was titrated with 0.025 M NaOH until pH 11 was reached.

Because pH is temperature sensitive, mV was used as the measuring unit during the titrations instead of pH to secure stabile measuring. pH and mV is proportional, and a trend line was drawn from three pH values at 4, 7 and 10 and the equivalent mV values.

3.6 Calibration Curve for Genistein and Daidzein

A result from a HPLC-analyzed sample is presented in area (i.e., the area under the relevant peak in the chromatogram). A calibration curve is necessary to transform the HPLC results from area to concentration. By analyzing samples with known concentrations and getting the results in area, a calibration curve can be made by plotting area vs. concentration. The trend line for the points makes the conversion factor between area and concentration. Calibration standards are also needed to make sure from one experiment to another that the results are comparable. This is confirmed by the results as the calibration standards were consistent over time.

Seven genistein solutions were made by spiking 10 µL to 500 µL of the 10 mM genistein stock solution into 10 mL deionized water. The resulting genistein concentrations were 1, 2, 5, 10, 15, 25 and 50 µM. A seven point calibration curve was made by analyzing the seven samples on the HPLC at 259 nm. The exact same procedure was followed for daidzein, but with at a wavelength of 249 nm instead of 259 nm.

3.7 Isotherm Experiments

Adsorption isotherms for genistein and daidzein onto goethite were obtained using standard batch sorption experiments at room temperature (24 °C.).

In seven small numbered glass bottles, 0.2 g goethite were mixed with 20 mL MOPS buffer solution to get a solid-to-water ratio in each bottle of 10 g/L. A control bottle without goethite was made in an eighth glass bottle with only 20 mL MOPS buffer. The pH was measured and adjusted to 5.5 +/- 0.1 with HCl and NaOH. The eight bottles were sealed and put on a shaker table for prewetting over night. The next morning, seven different volumes of the 0.001 M genistein stock solution were spiked into the first seven bottles to get concentrations varying from 0.0945 mg/L to 1.485 mg/L (0.35 µM – 5.5 µM) genistein. The same amount of genistein was spiked in the control bottle as in bottle nr. 3. The pH was measured again and the bottles were stored in a dark box on a shaker table for 72 hours. The bottles were then taken of the shaker table and the pH was measured one last time. Approximately 1.5 mL was removed from each bottle and centrifuged for 10 minutes at 15 000 rpm, to separate the goethite particles from the solution. The supernatants were pipetted into HPLC-vials and capped. The vials were analyzed in the HPLC at 259 nm together with some of the known calibration curve standards. This was done to ensure that the results were comparable from experiment to experiment.

The isotherm experiments were conducted three more times at different pH values (6.2, 7.1 and 8.2). The same procedure was repeated for daidzein, with a few changes. The concentrations of daidzein in the bottles varied from 0.102 mg/L to 1.5045 mg/L (0.4 µM – 1.6 µM). The exact concentrations of both genistein and daidzein may be seen in the appendix (chapter 8.1). Also the supernatants were analyzed at 249 nm instead of 259 nm. In Figure 3-3, the bottles from an isotherm experiment with genistein and daidzein are shown.

Figure 3-3: Bottles with goethite, MOPS buffer and one of the phytoestrogens, daidzein or genistein.

3.8 Sorption Edge Experiments

Sorption edge experiments for genistein and daidzein onto goethite were obtained using standard batch sorption experiments at 24 °C. The experiments were very similar to the isotherms experiments. Instead of varying the concentrations in all the bottles, however, the concentrations were kept constant with varying pH.

In nine glass bottles 0.1 g goethite was mixed with 10 mL MOPS buffer solution to get a solid-to-water ratio in each bottle of 10 g/L. The pH was adjusted by using HCl and NaOH to approximately 4.5, 7.25, 7.5, 7.75, 8.0, 8.5, 9.0, 9.5 and 10. The bottles were sealed and put on a shaker table for prewetting over night. The morning after, 37 µL of the 10 mM genistein stock solution were spiked into each bottle to get a concentration of 1 mg/L (3.7 µM) genistein. Afterwards, the pH was measured once again and the bottles were put in a dark box on the shaker table for 72 hours. Subsequent treatment was identical to that for the isotherm experiments.

Duplicates were made of all the bottles. Control batches without goethite were also made for each pH. Nine control samples were taken from the control batches directly after the adding of genistein. Another nine samples were taken 72 hours later at equilibrium. The nine samples taken at equilibrium were centrifuged before being analyzed in the HPLC. The remaining nine samples were not centrifuged. This was done to check the consistency in the control samples from start to beginning of the experiment. The same procedure was repeated for daidzein. Daidzein (39 µL) was spiked in each bottle to reach a concentration of 1 mg/L (3.9 µM).

4. Results and Discussion

4.1 Calculation of SSA_{TEM} for goethite

Based on the equations in section 3.2.1, the SSA_{TEM} was calculated from the average of 500 particles to be 248 $m^2/g \pm 90$ m^2/g. SSA_{BET} was measured as 118.5 $m^2/g \pm 2,6$ m^2/g. The SSA_{BET} is assumed to be more accurate than SSA_{TEM} because fine surface structures are included in the SSA_{BET} measurements. This feature will usually result in a higher SSA than if calculated from TEM pictures. In this case, however, it is the other way around, where the SSA_{TEM} is twice as high as SSA_{BET}. This may be explained with smaller particles than average on the images shot with the TEM. Furthermore, smaller particles are easier to keep track of and count because they do not "disappear" into areas full of particles, which may have promoted the counting of smaller particles rather than large ones. In general, SSA varies a lot, because of different size distributions from sample to sample. Differences in SSA will also affect the density of surface functional groups. A higher SSA results in a higher density of surface functional groups.

The SSA_{BET} of 118,5 $m^2/g \pm 2,6$ m^2/g is used in subsequent calculations regarding pK_a, adsorption isotherms and sorption edges.

4.1 Calculation of pK_a values for goethite

A calibration curve for mV and pH was made from measurements of pH 4, 7 and 10 standards, and the corresponding mV values. This was done to secure stabile measuring through the experiment, using mV instead of pH because pH is temperature sensitive. The correlation for the points is seen in Figure 4-1.

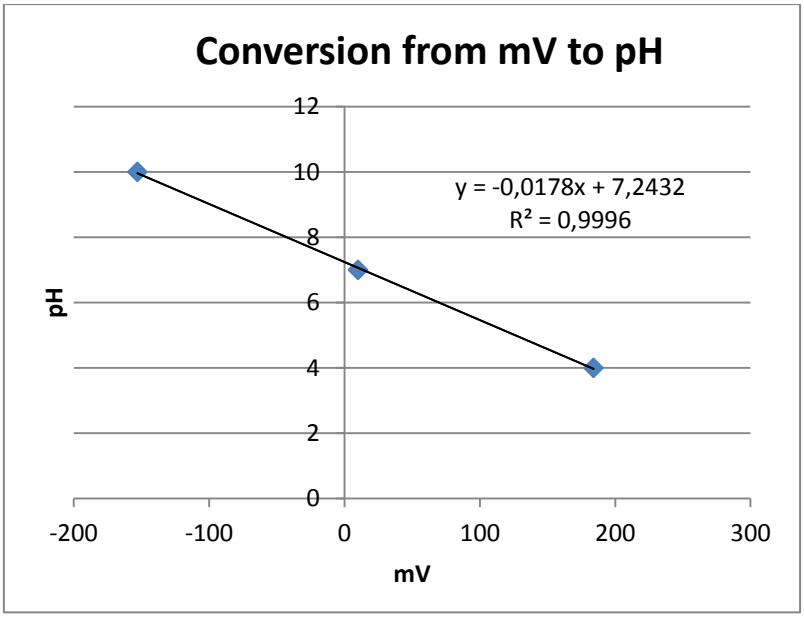

Figure 4-1: pH vs. mV, with the conversion factor from mV to pH.

The trend line makes the conversion factor, written in Equation 4.1, while the R^2 value indicates an approximated perfect correlation.

(4.1) pH = -0.0178 * mV + 7.2432

The pK_a values for goethite were calculated from the results of the titration, through the following steps. The experimental titration curve is shown in Figure 4-2 and the associated data are found in the appendix (Section 7.4).

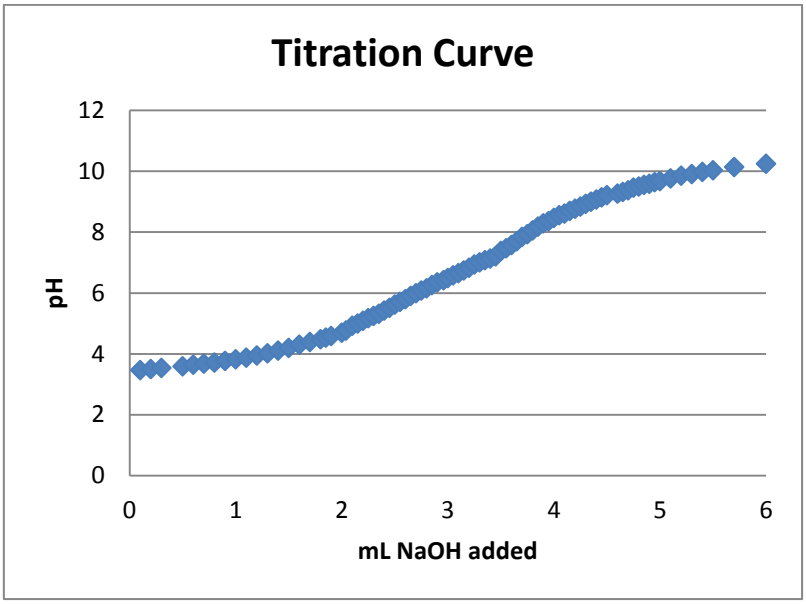

Figure 4-2: Titration curve made from pH vs. mL of NaOH added.

The mean surface charge (Q) of the particles was calculated from Equation 4-2. Q is measured in mol/kg.

(4.2) $$Q = \frac{C_A - C_B + [OH^-] - [H^+]}{a}$$

C_A and C_B are the concentrations of HCl and NaOH, respectively, in the solution (M). $[H^+]$ and $[OH^-]$ are calculated from the measured pH (M), and *a* is the amount of goethite in the solution, measured in kg/L. Q changes with pH, which is shown in Figure 4-3.

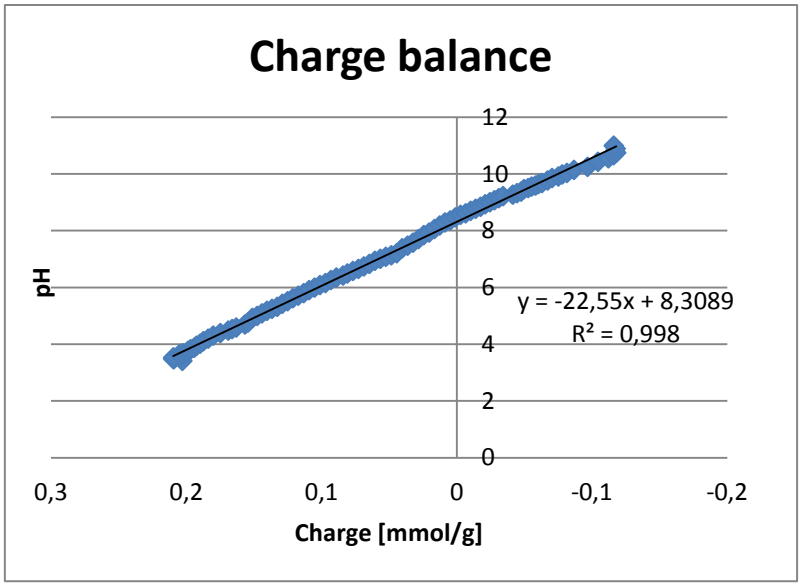

Figure 4-3: Charge of the solution plotted against increasing pH. At the intersection with the Y-axis is the point of zero charge (pH_{pzc})

The pH of point zero charge, pH_{pzc}, for goethite was found at the intersection on the y-axis at pH 8.3. It is a bit higher than previously observed values pH 7.8 (Brezonik and Arnold, 2011) and 7.9 (Stumm and Morgan, 1995).

With the mean surface charge calculated, the pK_a values were calculated using the following equations. Equation 4.3 and 4.4 show how to calculate K^s_{a1} and K^s_{a2}, respectively.

(4.3) $$K^s_{a1} = \frac{((TOT \equiv FeOH) - Q) * [H^+]}{Q}$$

(4.4) $$K^s_{a2} = \frac{Q * [H^+]}{(TOT \equiv FeOH) - Q}$$

TOT≡FeOH is the concentration of surface functional groups in mol/g, and is in Stumm and Morgan (1995) determined to 0.0002 mol/g. The goethite used in these experiments had a much higher SSA than the goethite used for the experiments in the book. On background of calculations, the concentration of the surface functional groups were estimated to be four times as high, 0.0008 mol/g. Equation 4.3 applies for pH lower than pH_{pzc}, while Equation 4.4 applies for pH higher than pH_{pzc}. K^s_{a1} and K^s_{a2} are transformed through multiplying with the negative logarithm to pK^s_{a1} and pK^s_{a2}. An absolute value of Q must be used in calculating pK_{a2} because logarithm cannot be applied on a negative number. This is also justified by the improbable unit of negative mol/kg.

The pK^s_{a1} and pK^s_{a2} values were plotted against Q as seen in Figure 4-4. Linear trend lines were made for both pK^s_{a1} and pK^s_{a2}, and the intersection with the Y-axis marks the pK_a values for goethite at 6.73 and 10.34, respectively.

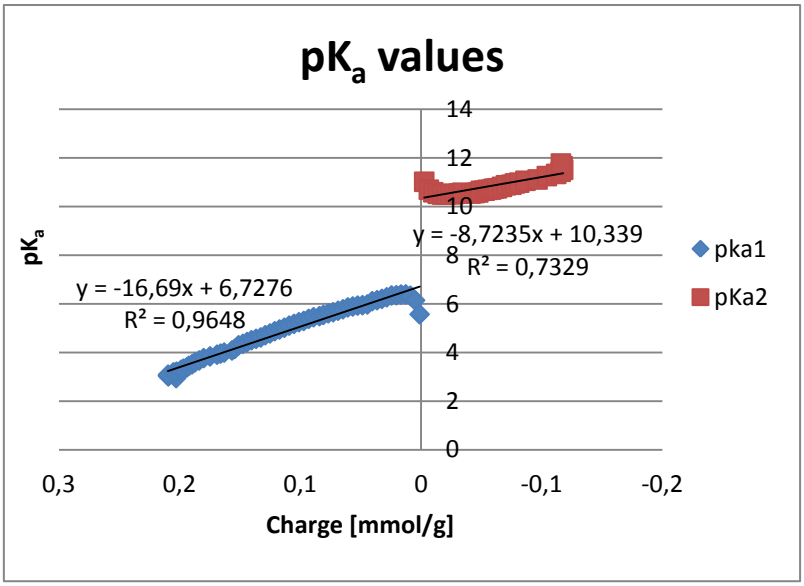

Figure 4-4: pK$_a$ plotted against the charge of the molecules. The intersection between the trend lines and the y-axis show the pK$_a$ values.

There may be some uncertainties related to these results due to lack of replicates.

4.2 Calibration Curve for Genistein and Daidzein

The unprocessed data that the calibration curves are based on is found in the appendix, Section 7.1. The calibration curve for genistein made in advance of the isotherm and sorption edge experiments is seen in Figure 4-5.

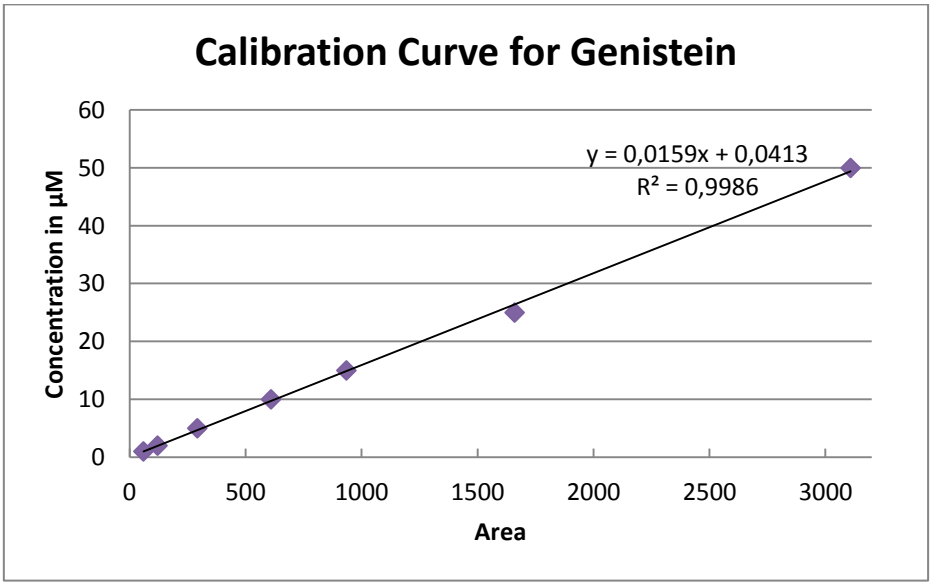

Figure 4-5: Calibration curve for genistein with the conversion factor between area and concentration.

The conversion factor from area to concentration was determined by the regression line formula shown in Figure 4-5. The formula is shown in Equation 4.5

(4.5) Concentration (µM) = 0.0197 * Area + 0.247

The equivalent calibration curve for daidzein is shown in Figure 4-6.

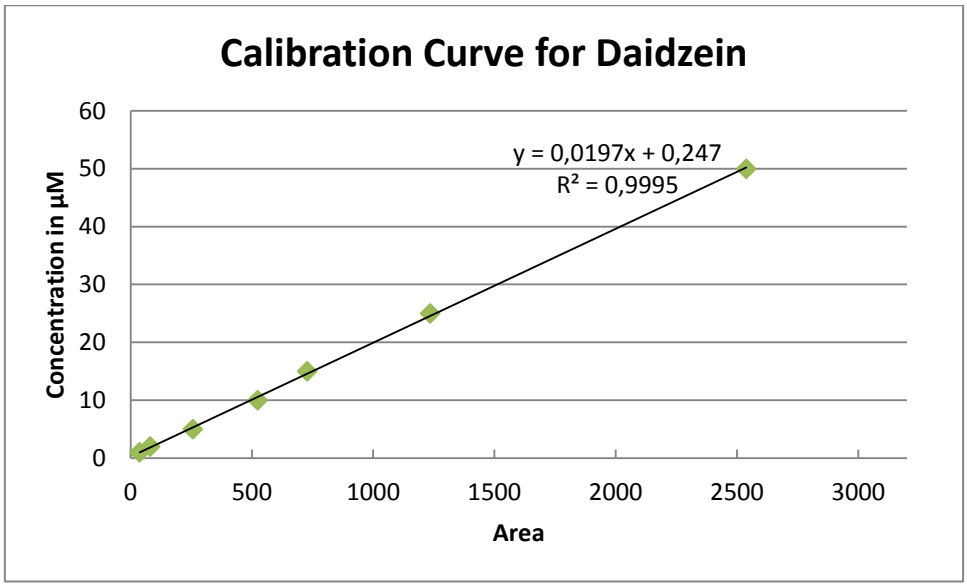

Figure 4-6: Calibration curve for daidzein with the conversion factor between area and concentration.

The trendline makes the conversion factor from area to concentration for daidzein. The conversion equation is shown in Equation 4.6.

(4.6) Concentration = 0.0197 * Area + 0.247

The conversion factor was used to convert the area outputs from the HPLC to concentrations. Both calibration curves show a good correlation between area and concentration. The calibration curves, adsorption isotherms and sorption edges are made from the same stock solutions of genistein and daidzein, which makes the areas and concentrations comparable.

4.3 Adsorption Isotherms and Sorption Edges for Daidzein and Genistein

The unprocessed data from the adsorption isotherms can be found in the appendix (Section 7.2). The adsorption isotherms for genistein and daidzein were calculated from Equation 2.4 and 2.5 and are presented in Figure 4-7 and 4-8, respectively. The four isotherms made for each compound at different pH are showed together.

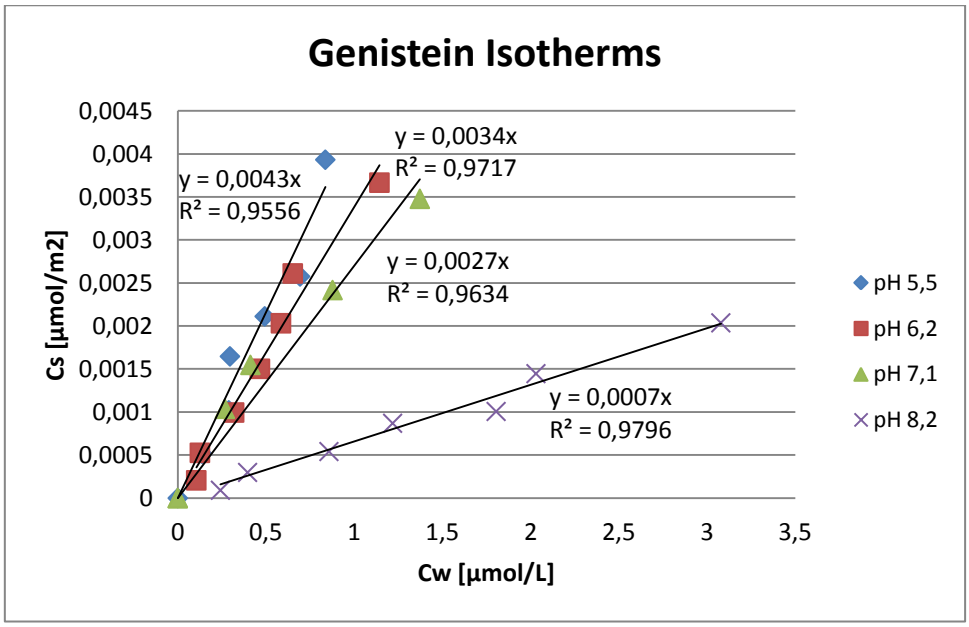

Figure 4-7: Four isotherms for genistein at different pH values.

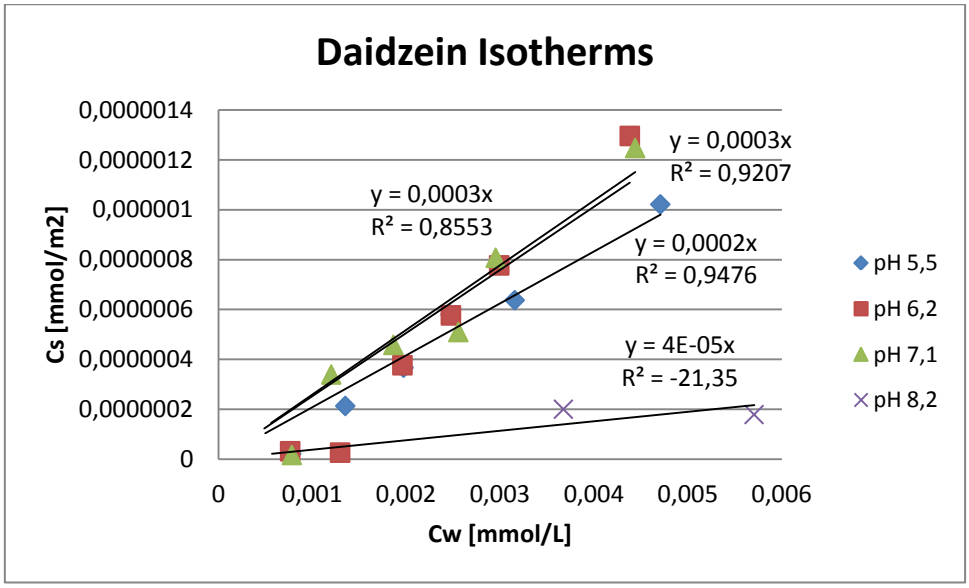

Figure 4-8: Four isotherms for daidzein at different pH values.

All the isotherms, except daidzein at pH 8.2, show clear linear correlations and linear trendlines were made due to this. This linear correlation suggests that concentration changes of genistein and daidzein have no considerable effect on goethite within these environmental relevant adsorbate concentrations. The slopes of the isotherms indicate the adsorption coefficients, K_D in L/m^2, which are shown in Table 4-1.

Table 4-1: K_D for genistein and daidzein at different pH from isotherm experiments.

Compound	pH	K_D [L/m^2]
GEN	5.5	0.0043
GEN	6.2	0.0034
GEN	7.1	0,0027
GEN	8.2	0,0007
DDZ	5.5	0,0002
DDZ	6.2	0.0003
DDZ	7.1	0.0003

Both the table and the isotherms show that genistein has a higher adsorption coefficient than daidzein. Based on calculations of the results, approximately 80 % of the total mass of genistein was adsorbed independent of the initial concentration. The mass percent of daidzein adsorbed, however, is only 20 % of the initial mass. This is true for pH 5.5, 6.2 and 7.1. At pH 8.2, however, K_D is much lower for genistein. For daidzein at pH 8.2 it was practically impossible to get a reasonable K_D because nothing was adsorbed, and most of the final daidzein concentrations were measured a little higher than the initial concentrations. It indicates that the daidzein stock solution, which is used for the isotherms, might be just a little inaccurate. The problem with slightly higher final concentrations could have been avoided with a control sample for every sample made. C_S could then have been calculated from the actual initial concentration instead of the assumed initial concentration.

The isotherms at pH 8.2 are noticeably different from the other pH values, which suggest that something is happening between pH 7.1 and 8.2. The sorption edges were made from pH 4.8 to pH 10, but with more frequent samples in the pH area stretching from 7.1 to 8.2. They are calculated on the basis of Equation 2.4, 2.5 and 2.10. The sorption edge for genistein is seen in Figure 4-9, while it is seen for daidzein in Figure 4-10. They show how K_D varies with pH. The K_D values from the isotherm experiments are included in the sorption edge graphs.

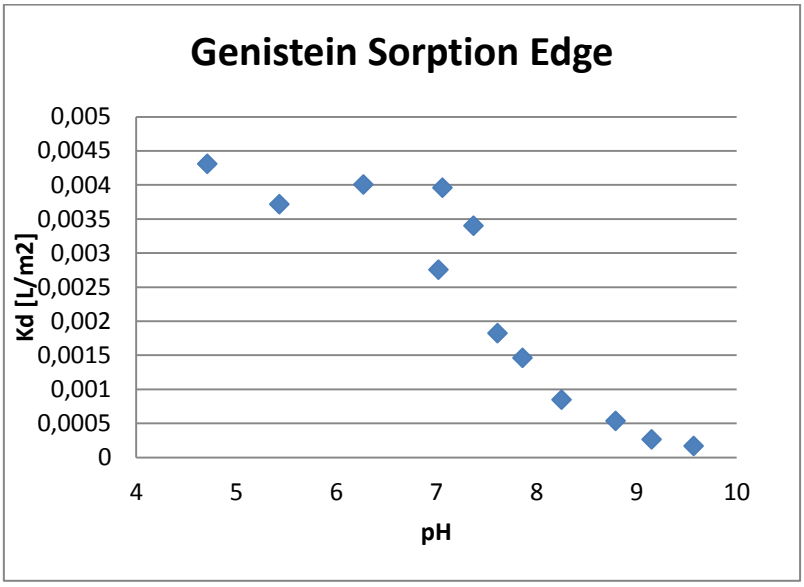

Figure 4-9: Sorption edge for genistein at a concentration of 1 mg/L.

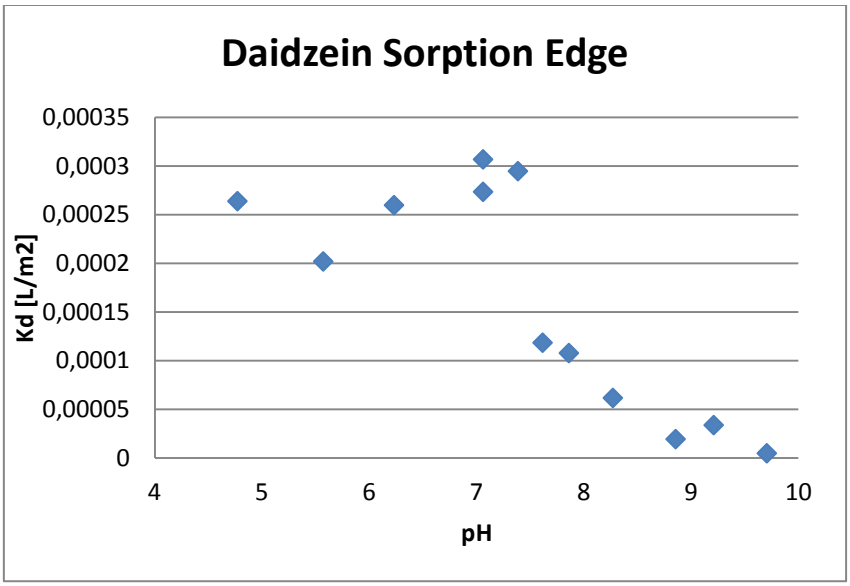

Figure 4-10: Sorption edge for daidzein at a concentration of 1 mg/L.

Figure 4-9 and 4-10 show that adsorption of both phytoestrogens onto goethite is dependent on pH. The general tendency is that K_D decreases with pH. The K_D values and the percent mass adsorbed at the different pH are presented in Table 4-2 to give an overview. Only the results from the sorption edge experiments are included in Table 4-2, and not the K_D values from the isotherm experiments.

Table 4-2: K_D and percent mass adsorbed for genistein and daidzein at different pH from sorption edge experiments.

Compound	pH	K_D [L/m^2]	Percent mass adsorbed [%]
GEN	4.7	0.00431	84
GEN	7,1	0.00396	82
GEN	7,4	0.003401	80
GEN	7,6	0.001824	68
GEN	7,9	0.001461	63
GEN	8,2	0.000847	50
GEN	8,8	0.000536	39
GEN	9.1	0.000265	24
GEN	9.6	0.000168	17
DDZ	4.7	0.000264	24
DDZ	7.1	0.000307	27
DDZ	7.4	0.000295	26
DDZ	7.6	0.000118	12
DDZ	7,9	0.000108	11
DDZ	8.3	6.15425E-05	7
DDZ	8.9	1.92297E-05	2
DDZ	9.2	3.36379E-05	4
DDZ	9.7	4.66691E-06	1

From Table 4-2 it is seen that K_D for genistein decreases continuously, while daidzein reaches a maxima of K_D at pH 7.1. This statement takes only the sorption edge experimental results into consideration, and not the K_D values from the isotherm experiment.

A radical decrease in K_D for both phytoestrogens is seen above pH of 7.4 and continues to the endpoint at pH 9.7. Daidzein adsorbs more poorly to goethite than genistein, and experiences practically no adsorption at pH 9.7. Electrostatic repulsion might be the reason for low adsorption at this pH. The goethite has a net negative surface charge when pH exceeds 8.3. The pK_{a2} value of daidzein at 9.7 supports this theory further. At pH 9.7 daidzein is dominated by the deprotonated DDZ^{2-}form. It is likely the same mechanism for genistein at high pH values, even though the pK_{a2} for genistein has not been reached yet at pH 9.7. Due to the lack of results at higher pH it is difficult to make further assumptions.

There is clearly an interaction at low pH between the protonated goethite and the fully protonated genistein and daidzein. A possible explanation is that daidzein and genistein, due to hydrophobicity, adsorb non-specifically to goethite to avoid or minimize contact with water. Another possible mechanism at low pH is that fully protonated states of genistein and daidzein forms surface complexes with the goethite.

Additional, fits for the sorption edges were made and modeled by Ms. Kelly using the software Scientist and they are seen in Figure 4-11. The adsorption capacity, C_S (mol/m^2), is used as the y-axis instead of K_D (L/m^2).

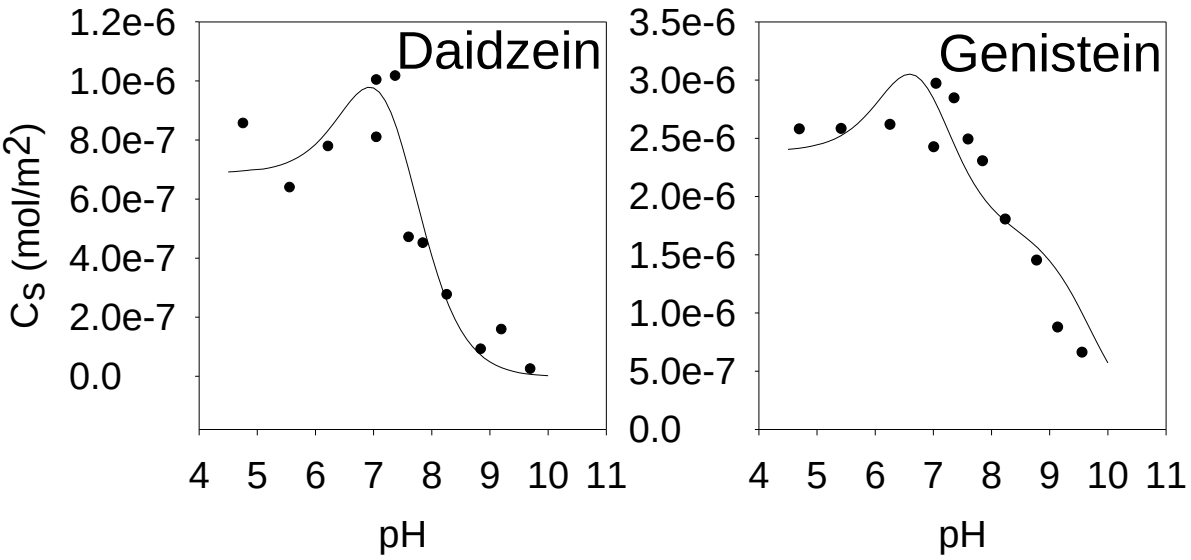

Figure 4-11: Sorption edges and their fits.

The fits were made in Scientist by feeding it with data (pH and C_S in this case) together with premade equations that includes parameters able to be fitted (K_1, K_2 and K_3). Scientist finds values for the fitting parameters, and comes up with a line of the best fit. The premade formulas for this fit were made by Ms. Kelly and are seen in Equation 4.7 and 4.8. Equation 4.7 applies for daidzein and Equation 4.8 for genistein.

(4.7) $$C_s = K_1[FeOH_2^+][H_2DDZ] + K_2[FeOH_2^+][HDDZ^-]$$

(4.8) $$C_s = K_1[FeOH_2^+][H_3GEN] + K_2[FeOH_2^+][H_2GEN^-] + K_3[FeOH_2^+][HGEN^{2-}]$$

Further fitting using the software FITEQL is planned by Ms. Kelly to get a better understanding. The results will be published late 2012 or early 2013.

The sorption edges in Figure 4-11 have a somewhat different expression than the sorption edges in Figure 4-9 and 4-10, because C_S is used as the y-axis instead of K_D. The most important feature in Figure 4-11 is the fits, however, which show the tendency of the sorption capacity at increasing pH. The fits seem to agree with the observations already made.

These results can be applied, to give an indication of the fate of phytoestrogens in the environment. In an aquatic environment containing goethite, both phytoestrogens will be removed by adsorption to a certain degree dependent on pH. Since the adsorption process is independent of the adsorbate

concentration, pH is the single factor that determines the adsorption capacity of the goethite. It is important to bear in mind, however, that many more factors are present in the environment than in these experiments, which must be taken into account.

More experiments should be done, to understand the adsorption mechanism better. Preferably at a bigger pH-range, to get more insight to the genistein adsorption mechanism especially. Also the rate of adsorption is environmentally interesting with regards to rivers. New experiments should also make sure to have a control sample for each sample, so C_S can be calculated from the actual initial concentration and not the assumed. The isotherm for daidzein at 8.2 might have looked different with control samples for all the samples.

5. Conclusion

SSA_{TEM} of the goethite nanoparticles was found to be 248 $m^2/g \pm 90$ m^2/g, while SSA_{BET} was measured to 118.5 $m^2/g \pm 2.6$ m^2/g. Furthermore the pK_a values for goethite were calculated at pH 6.73 and 10.34, and the pH_{pzc} were found at 8.3.

The isotherms indicated that the adsorption of genistein and daidzein onto goethite is independent of the concentrations at these environmental relevant concentrations. In addition, the sorption edge experiments for genistein and daidzein showed that the adsorption onto goethite is pH-dependent. For genistein the adsorption decreased constantly with increasing pH. The highest adsorption capacity was found at pH 4.7 with a K_D at 0.00431 L/m^2 and a percent mass adsorbed at 84 %. At pH higher than 7.4, the adsorption capacity started decreasing more rapidly, to a minimum of 17 % mass adsorbed and a K_D of 0.000168 L/m^2 at pH 9.7. Daidzein was only removed to a certain degree and had an adsorption maxima at pH 7.4, with 27 % mass adsorbed and a K_D at 0.000307 L/m^2. K_D and the percent mass adsorbed were slightly lower from pH 4.7 to 7.4. The minimum adsorption capacity for daidzein was found at pH 9.7, with a KD of 4.66691E-06 L/m^2 and only 1 % mass adsorbed.

It was suggested that hydrophobic interactions or surface complexations are the adsorption mechanisms at low pH for both genistein and daidzein. Electrostatic repulsion was proposed to be the reason for the drop in adsorption capacity at higher pH, when the compounds get deprotonated.

When using these results to predict the fate of genistein and daidzein in the environment, it is important to remember that many other factors present in the nature may play a role. The general picture though, is that genistein will be removed by adsorption to a greater extent than daidzein, when released to ferruginous natural waters. The removal of the phytoestrogens from the water phase through adsorption is also more relevant at low pH than high. In other words, adsorption as a removal mechanism of genistein and daidzein in natural waters is possible under certain circumstances. At low pH, the removal of genistein may be significant.

For better understanding of the adsorption mechanism further experiments should be done, particularly regarding the rate of adsorption.

6. References

ANSCHUTZ, A. J. & PENN, R. L. 2005. Reduction of crystalline iron(III) oxyhydroxides using hydroquinone: Influence of phase and particle size. *Geochemical Transactions,* 6**,** 60-66.

ARDIA, D. R. & CLOTFELTER, E. D. 2006. The novel application of an immunological technique reveals the immunosuppressive effect of phytoestrogens in Betta splendens. *Journal of Fish Biology,* 68**,** 144-149.

ARNOLD, W. A. 2012. *RE: Personal communication.*

BREZONIK, P. L. & ARNOLD, W. A. 2011. *Water chemistry: an introduction to the chemistry of natural and engineered aquatic systems,* Oxford, Oxford University Press.

CHUN, C. L., PENN, R. L. & ARNOLD, W. A. 2006. Kinetic and microscopic studies of reductive transformations of organic contaminants on goethite. *Environmental Science & Technology,* 40**,** 3299-3304.

CLOTFELTER, E. D. & RODRIGUEZ, A. C. 2006. Behavioral changes in fish exposed to phytoestrogens. *Environmental Pollution,* 144**,** 833-839.

FIGUEROA, R. A. & MACKAY, A. A. 2005. Sorption of oxytetracycline to iron oxides and iron oxide-rich soils. *Environmental Science & Technology,* 39**,** 6664-6671.

HOCHELLA JR, M. F., WIGGINGTON, N. S. & HAUS, K. L. 2007. Aquatic environmental nanoparticles. *Journal of environmental monitoring* 9**,** 1306-1316.

KAWANISHI, M., TAKAMURA-ENYA, T., ERMAWATI, R., SHIMOHARA, C., SAKAMOTO, M., MATSUKAWA, K., MATSUDA, T., MURAHASHI, T., MATSUI, S., WAKABAYASHI, K., WATANABE, T., TASHIRO, Y. & YAGI, T. 2004. Detection of genistein as an estrogenic contaminant of river water in Osaka. *Environmental Science & Technology,* 38**,** 6424-6429.

KELLY, M. M. & ARNOLD, W. A. 2012. Direct and Indirect Photolysis of the Phytoestrogens Genistein and Daidzein. *Environmental Science & Technology,* 46**,** 5396–5403.

KIPARISSIS, Y., BALCH, G. C., METCALFE, T. L. & METCALFE, C. D. 2003. Effects of the isoflavones genistein and equol on the gonadal development of Japanese medaka (Oryzias latipes). *Environmental Health Perspectives,* 111**,** 1158-1163.

KIPARISSIS, Y., HUGHES, R., METCALFE, C. & TERNES, T. 2001. Identification of the isoflavonoid genistein in bleached kraft mill effluent. *Environmental Science & Technology,* 35**,** 2423-2427.

KOLPIN, D. W., HOERGER, C. C., MEYER, M. T., WETTSTEIN, F. E., HUBBARD, L. E. & BUCHELI, T. D. 2010. Phytoestrogens and Mycotoxins in Iowa Streams: An Examination of Underinvestigated Compounds in Agricultural Basins. *Journal of Environmental Quality,* 39**,** 2089-2099.

LATONNELLE, K., FOSTIER, A., LE MENN, F. & BENNETAU-PELISSERO, C. 2002. Binding affinities of hepatic nuclear estrogen receptors for phytoestrogens in rainbow trout (Oncorhynchus mykiss) and Siberian sturgeon (Acipenser baeri). *General and Comparative Endocrinology,* 129**,** 69-79.

LIANG, J., TIAN, Y. X., FU, L. M., WANG, T. H., LI, H. J., WANG, P., HAN, R. M., ZHANG, J. P. & SKIBSTED, L. H. 2008. Daidzein as an Antioxidant of Lipid: Effects of the Microenvironment in Relation to Chemical Structure. *Journal of Agricultural and Food Chemistry,* 56**,** 10376-10383.

LUND, T. D., MUNSON, D. J., HALDY, M. E., SETCHELL, K. D. R., LEPHART, E. D. & HANDA, R. J. 2004. Equol is a novel anti-androgen that inhibits prostate growth and hormone feedback. *Biology of Reproduction,* 70**,** 1188-1195.

LUNDGREN, M. S. & NOVAK, P. J. 2009. QUANTIFICATION OF PHYTOESTROGENS IN INDUSTRIAL WASTE STREAMS. *Environmental Toxicology and Chemistry,* 28**,** 2318-2323.

METCALF & EDDY, I., TCHOBANOGLOUS, G., BURTON, F. L. & STENSEL, H. D. 2003. *Wastewater engineering: treatment and reuse,* Boston, McGraw-Hill.

SIGMA-ALDRICH. *Catalog Search* [Online]. Sigma-Aldrich. Available: http://www.sigmaaldrich.com/norway.html [Accessed 7th of June 2012].

STEMIG, A. 2012. *RE: Personel communication.*

STUMM, W. & MORGAN, J. J. 1995. *Aquatic Chemistry: Chemical Equilibria and Rates in Natural Waters,* New York, Wiley.

THORPE, K. L., CUMMINGS, R. I., HUTCHINSON, T. H., SCHOLZE, M., BRIGHTY, G., SUMPTER, J. P. & TYLER, C. R. 2003. Relative potencies and combination effects of steroidal estrogens in fish. *Environmental Science & Technology,* 37**,** 1142-1149.

TRIBE, L. & BAJA, B. C. 2004. Adsorption of phosphate on goethite. *Journal of Chamical Education,* 81.

TURNER, J. V., AGATONOVIC-KUSTRIN, S. & GLASS, B. D. 2007. Molecular aspects of phytoestrogen selective binding at estrogen receptors. *Journal of Pharmaceutical Sciences,* 96**,** 1879-1885.

WYNNE-EDWARDS, K. E. 2001. Evolutionary biology of plant defenses against herbivory and their predictive implications for endocrine disruptor susceptibility in vertebrates. *Environmental Health Perspectives,* 109**,** 443-448.

ZIELONKA 2003. Radical scavenging properties of genistein. *Free Radical Biology and Medicine* 35**,** 958.

7. Appendix

7.1 Unprocessed results from calibration curve experiments

Parallel 1			Parallel 2		
Sample	Area	Conc [µM]	Sample	Area	Conc [µM]
kD1 o1	38,1	1	kD1 o2	35,7	1
kD2 o1	83,2	2	kD2 o2	78,8	2
kD5 o1	257,4	5	kD5 o2	256,3	5
kD10 o1	523,9	10	kD10 o2	523,9	10
kD15 o1	730,4	15	kD15 o2	725,8	15
kD25 o1	1233	25	kD25 o2	1237,6	25
kD50 o1	2539,3	50	kD50 o2	2537,6	50
kG1 o1	59,9	1	kG1 o2	59,6	1
kG2 o1	121,3	2	kG2 o2	120,3	2
kG5 o1	294,4	5	kG5 o2	290,1	5
kG10 o1	615,3	10	kG10 o2	604,7	10
kG15 o1	938,6	15	kG15 o2	931,3	15
kG25 o1	1665,1	25	kG25 o2	1655,6	25
kG50 o1	3115,7	50	kG50 o2	3102	50

7.2 Unprocessed results from isotherm experiments

pH 5,5

Sample	Weight (g)	pH start	pH after a night	pH after 72 hours	µL	Start conc. [mg/L]	Start conc. [mmol/L]	Area
G1	0,1998	5,47	5,47		7	0,0945	0,000349689	Not measurable
G2	0,2001	5,49	5,45		15	0,2025	0,000749334	6,1
G3	0,2001	5,55	5,52		30	0,405	0,001498668	15,6
G4	0,2	5,47	5,43		45	0,6075	0,002248002	16
G5	0,2001	5,46	5,43		60	0,81	0,002997336	28,4
G6	0,2	5,47	5,43		75	1,0125	0,00374667	41
G7	0,1999	5,51	5,5		110	1,485	0,005495115	50
G8 (control)	0	5,39	5,36		45	0,405	0,001498668	119,9
D1	0,2	5,5	5,48		8	0,102	0,000401196	12,8
D2	0,2001	5,52	5,47		16	0,204	0,000802391	26,9
D3	0,2001	5,52	5,47		32	0,408	0,001604783	56,1
D4	0,2	5,5	5,48		48	0,612	0,002407174	87,6
D5	0,2	5,59	5,57		63	0,8033	0,003159613	113
D6	0,2	5,52	5,47		78	0,9945	0,003911658	147,7
D7	0,2	5,53	5,51		118	1,5045	0,005917637	226,4
D8 (control)	0	5,51	5,48		48	0,408	0,001604783	106

pH 6,2

Sample	Weight (g)	pH start	pH after a night	pH after 72 hours	µL	Start conc. mg/L	Start conc. [mmol/L]	Area
G1	0,2	6,25	6,26		7	0,0945	0,000349689	4
G2	0,2	6,21	6,21		15	0,2025	0,000749334	5,3
G3	0,2	6,23	6,24		30	0,405	0,001498668	17,5
G4	0,2001	6,21	6,24		45	0,6075	0,002248002	26,7
G5	0,2003	6,22	6,24		60	0,81	0,002997336	34,2
G6	0,2	6,26	6,27		75	1,0125	0,00374667	38,4
G7	0,2003	6,23	6,24		110	1,485	0,005495115	69,3
G8 (control)	0	6,23	6,25		45	0,405	0,001498668	123,4
D1	0,2	6,22	6,19		8	0,102	0,000401196	12,2
D2	0,2002	6,21	6,21		16	0,204	0,000802391	26,3
D3	1,999	6,26	6,24		32	0,408	0,001604783	53,3
D4	0,2001	6,24	6,22		48	0,612	0,002407174	87
D5	0,1999	6,23	6,22		63	0,8033	0,003159613	113,2
D6	0,2	6,25	6,23		78	0,9945	0,003911658	139,3
D7	0,2	6,24	6,23		118	1,5045	0,005917637	209,9
D8 (control)	0	6,23	6,22		48	0,408	0,001604783	118,1

pH 7,1

Sample	Weight (g)	pH start	pH after a night	pH after 72 hours	µL	Starting conc. mg/L	Start conc. [mmol/L]	Area
G1	0,2	7,12	7,13		7	0,0945	0,000349689	Not measurable
G2	0,2002	7,1	7,07		15	0,2025	0,000749334	Not measurable
G3	0,2002	7,12	7,04		30	0,405	0,001498668	14,2
G4	0,2001	7,07	7,03		45	0,6075	0,002248002	23,3
G5	1,999	7,08	7,04		60	0,81	0,002997336	42,9
G6	0,2002	7,09	7,05		75	1,0125	0,00374667	52,6
G7	0,2	7,06	7,02		110	1,485	0,005495115	83,7
G8 (control)	0	7,1	7,05		45	0,405	0,001498668	99,9
D1	0,2001	7,08	7,03		8	0,102	0,000401196	15,8
D2	0,2	7,09	7,04		16	0,204	0,000802391	27,2
D3	0,2002	7,12	7,06		32	0,408	0,001604783	48,5
D4	0,2	7,12	7,05		48	0,612	0,002407174	82,1
D5	0,2	7,12	7,07		63	0,8033	0,003159613	117,2
D6	0,2002	7,12	7,06		78	0,9945	0,003911658	137,4
D7	0,2	7,12	7,05		118	1,5045	0,005917637	212,8
D8 (control)	0	7,09	7,02		48	0,408	0,001604783	108

pH 8,2

Sample	Weight (g)	pH start	pH after a night	pH after 72 hours	µL	Start conc. mg/L	Start conc. [mmol/L]	Area
G1	0,2	8,41	8,31		7	0,0945	0,000349689	12,6
G2	0,2	8,26	8,17	8,18	15	0,2025	0,000749334	22,3
G3	0,2001	8,46	8,32		30	0,405	0,001498668	51,3
G4	0,1999	8,44	8,28	8,29	45	0,6075	0,002248002	74
G5	0,1999	8,51	8,42		60	0,81	0,002997336	110,9
G6	0,2002	8,38	8,23	8,24	75	1,0125	0,00374667	125,1
G7	0,2002	8,63	8,44		110	1,485	0,005495115	191
G8 (control)	0	8,33	8,25	8,25	45	0,405	0,001498668	131,5
D1	0,2	8,21	8,2	8,21	8	0,102	0,000401196	16,3
D2	0,1998	8,5	8,39		16	0,204	0,000802391	36,9
D3	1,999	8,24	8,18	8,18	32	0,408	0,001604783	73,2
D4	0,2001	8,3	8,24		48	0,612	0,002407174	113,1
D5	0,2001	8,33	8,23	8,21	63	0,8033	0,003159613	155,5
D6	0,1999	8,21	8,12		78	0,9945	0,003911658	174
D7	0,2001	8,32	8,2		118	1,5045	0,005917637	277,1
D8 (control)	0	8,37	8,29	8,3	48	0,408	0,001604783	117,7

7.3 Unprocessed results from sorption edge experiments

Daidzein

Conc of DDZ (Co)	0,9945	mg/L
	0,00391	mmol/L
Volume of DDZ added	39	µL
Volume of MOPS	0,01	L
Conversion factor	y=0,0197x+0,247	

1st Parallel

Sample	Weight (g)	pH start	pH after 1 night	pH after 3-4 days	Area
1Da	0,1	4,5	4,7	4,72	147,7
2Da	0,1001	7,26	7,1	7,06	150,9
3Da	0,1	7,5	7,41	7,36	162,2
4Da	0,1001	7,78	7,69	7,61	191,2
5Da	0,1	8,04	7,95	7,86	198,5
6Da	0,1001	8,5	8,38	8,31	214,2
7Da	0,1001	9,08	8,93	8,9	223,3
8Da	0,0999	9,56	9,3	9,22	227,6
9Da	0,1	10,01	9,77	9,65	228,9

2nd Parallel

Sample	Weight (g)	pH start	pH after 1 night	pH after 3-4 days	Area
1Db	0,1	4,53	4,73	4,77	156,11
2Db	0,1001	7,25	7,12	7,06	155,5
3Db	0,1	7,55	7,46	7,41	162,5
4Db	0,0999	7,79	7,69	7,62	186
5Db	0,1	8,05	7,95	7,86	199,7
6Db	0,1	8,47	8,32	8,23	213
7Db	0,1001	9,09	8,88	8,81	225,1
8Db	0,1	9,49	9,29	9,2	219,2
9Db	0,1001	10,06	9,86	9,76	234

Control samples without goethite taken and stored the first day (not centrifuged)

Sample	Weight (g)	pH start	pH after 1 night	pH after 3-4 days	Area
1Dca	0	4,42	.	.	207,4
2Dca	0	7,28	.	.	216,2
3Dca	0	7,55	.	.	227,7
4Dca	0	7,76	.	.	219,4
5Dca	0	8,03	.	.	228,5
6Dca	0	8,48	.	.	232,5
7Dca	0	8,99	.	.	232,3
8Dca	0	9,57	.	.	236
9Dca	0	9,96	.	.	234,9

Control samples without goethite taken the last day (centrifuged)

Sample	Weight (g)	pH start	pH after 1 night	pH after 3-4 days	Area
1Dcb	0	4,42	4,47	4,52	203,3
2Dcb	0	7,28	7,13	7,08	213,5
3Dcb	0	7,55	7,42	7,3	223,4
4Dcb	0	7,76	7,68	7,6	216,8
5Dcb	0	8,03	7,95	7,81	226,1
6Dcb	0	8,48	8,38	8,27	230,1
7Dcb	0	8,99	8,83	8,6	229,6
8Dcb	0	9,57	9,38	9,16	232,8
9Dcb	0	9,96	9,81	63	232,8

Control samples without goethite taken on the last day of the exp. (not centrifuged)

Sample	Weight (g)	pH start	pH after 1 night	pH after 3-4 days	Area
4Dcc	0	7,76	7,68	7,6	219,2
7Dcc	0	8,99	8,83	8,6	231,3

Genistein

Conc of GEN (Co	1	mg/L
	0,0037	mM
Volume of GEN added	37	µL
Volume of MOPS	0,01	L
Conversion factor	y=0,0159x+0,0413	

1st parallel

Sample	Weight (g)	pH start	pH after 1 night	pH after 3-4 days	Area
1Ga	0,1002	4,52	4,69	4,76	31,2
2Ga	0,1001	7,28	7,12	7,1	47,7
3Ga	0,1	7,52	7,4	7,36	51,3
4Ga	0,1	7,79	7,67	7,61	83,3
5Ga	0,1001	8,02	7,92	7,86	95,7
6Ga	0,1001	8,44	8,25	8,18	124,6
7Ga	0,1001	9,05	8,85	8,76	167,1
8Ga	0,1	9,55	9,22	9,1	204,2
9Ga	0,1	9,96	9,74	9,66	243,1

2nd parallel

Sample	Weight (g)	pH start	pH after 1 night	pH after 3-4 days	Area
1Gb	0,1001	4,48	4,65	4,71	38,7
2Gb	0,1	7,26	7,1	7,06	41,3
3Gb	0,1	7,53	7,42	7,37	48,5
4Gb	0,1001	7,78	7,67	7,61	82,9
5Gb	0,1	8,03	7,92	7,86	97
6Gb	0,1001	8,45	8,34	8,25	137,2
7Gb	0,1001	9,06	8,89	8,79	167,1
8Gb	0,1001	9,52	9,25	9,15	204,2
9Gb	0,1	10,04	9,81	9,57	243,1

Control samples without goethite taken and stored the first day (not centrifuged)					
Sample	**Weight (g)**	**pH start**	**pH after 1 night**	**pH after 3-4 days**	**Area**
1Gca	0	4,47	0	0	235,7
2Gca	0	7,32	0	0	277,6
3Gca	0	7,52	0	0	270,8
4Gca	0	7,77	0	0	275,6
5Gca	0	8,04	0	0	276,6
6Gca	0	8,45	0	0	268
7Gca	0	9	0	0	278
8Gca	0	9,57	0	0	267
9Gca	0	10	0	0	294

Control samples without goethite taken the last day (centrifuged)					
Sample	**Weight (g)**	**pH start**	**pH after 1 night**	**pH after 3-4 days**	**Area**
1Gcb	0	4,47	4,22	4,45	227
2Gcb	0	7,32	7,16	7,09	265,6
3Gcb	0	7,52	7,39	7,33	261,5
4Gcb	0	7,77	7,67	7,59	268,4
5Gcb	0	8,04	7,93	7,8	267,8
6Gcb	0	8,45	8,33	8,22	265,1
7Gcb	0	9	8,84	8,77	275
8Gcb	0	9,57	9,41	9,26	269,1
9Gcb	0	10	9,83	9,64	291,9

Control samples without goethite taken on the last day of the exp. (not centrifuged)					
Sample	**Weight (g)**	**pH start**	**pH after 1 night**	**pH after 3-4 days**	**Area**
4Dcc	0	7,77	7,67	7,59	237
7Dcc	0	9	8,84	8,77	278,7

7.4 Unprocessed results from titration experiments

1 parallel
0,1 M NaOH
0,2 M HCl

Grams of goethite: 0,147 g
Volume: 100 mL NaClO4

	mV	mL NaOH added	mL HCl added	pH
"Start"	11	0	0	7,0474
	155	0	0,5	4,4842
Start	173	0	0,7	4,1638
	161	0,2	0	4,3774
	153	0,3	0	4,5198
	128	0,5	0	4,9648
	95	0,7	0	5,5522
	68	0,9	0	6,0328
	54	1	0	6,282
	47	1,05	0	6,4066
	30	1,15	0	6,7092
	20	1,2	0	6,8872
	11	1,25	0	7,0474
	1	1,3	0	7,2254
	-11	1,35	0	7,439
	-26	1,4	0	7,706
	-36	1,45	0	7,884
	-48	1,5	0	8,0976
	-58	1,55	0	8,2756
	-67	1,6	0	8,4358
	-84	1,7	0	8,7384
	-90	1,75	0	8,8452
	-94	1,8	0	8,9164
	-99	1,85	0	9,0054
	-104	1,9	0	9,0944
	-110	1,95	0	9,2012
	-115	2	0	9,2902
	-119	2,05	0	9,3614
	-123	2,1	0	9,4326
	-127	2,15	0	9,5038
	-130	2,2	0	9,5572
	-134	2,25	0	9,6284
	-137	2,3	0	9,6818
	-139	2,35	0	9,7174
	-142	2,4	0	9,7708
	-144	2,45	0	9,8064
	-145	2,5	0	9,8242
	-148	2,55	0	9,8776
	-150	2,6	0	9,9132
	-152	2,65	0	9,9488
	-157	2,8	0	10,0378
	-161	2,9	0	10,109
	-166	3,1	0	10,198
	-172	3,3	0	10,3048
	-175	3,5	0	10,3582
	-178	3,6	0	10,4116
	-181	3,8	0	10,465
	-185	4	0	10,5362
	-189	4,3	0	10,6074
	-191	4,5	0	10,643
	-193	4,7	0	10,6786
	-196	5	0	10,732
	-201	5,5	0	10,821

-205	6	0	10,8922
-211	7	0	10,999
-216	8	0	11,088
-221	9	0	11,177
-224	10	0	11,2304
-227	11	0	11,2838
-230	12	0	11,3372
-232	13	0	11,3728
-237	15	0	11,4618
-240	17	0	11,5152
-244	20	0	11,5864

2 parallel
0,025 M NaOH
0,05 M HCl

Grams of goethite: 0,2942 g
Volume: 100 mL M NaClO4

	mV	mL NaOH added	mL HCl added	pH
"Start"	10	0	0	7,0652
	88	0	0,5	5,6768
	167	0	1	4,2706
	199	0	1,5	3,701
Start	215	0	2	3,4162
	212	0,1	2	3,4696
	210	0,2	2	3,5052
	208	0,3	2	3,5408
	205	0,5	2	3,5942
	202	0,6	2	3,6476
	200	0,7	2	3,6832
	198	0,8	2	3,7188
	195	0,9	2	3,7722
	192	1	2	3,8256
	189	1,1	2	3,879
	185	1,2	2	3,9502
	181	1,3	2	4,0214
	176	1,4	2	4,1104
	171	1,5	2	4,1994
	165	1,6	2	4,3062
	160	1,7	2	4,3952
	155	1,8	2	4,4842
	152	1,85	2	4,5376
	149	1,9	2	4,591
	143	2	2	4,6978
	139	2,04	2	4,769
	130	2,1	2	4,9292
	126	2,15	2	5,0004
	121	2,2	2	5,0894
	116	2,25	2	5,1784
	112	2,3	2	5,2496
	108	2,35	2	5,3208
	102	2,4	2	5,4276
	97	2,45	2	5,5166
	91	2,5	2	5,6234
	86	2,55	2	5,7124
	81	2,6	2	5,8014

75	2,65	2	5,9082
70	2,7	2	5,9972
65	2,75	2	6,0862
61	2,8	2	6,1574
55	2,85	2	6,2642
50	2,9	2	6,3532
46	2,96	2	6,4244
42	3	2	6,4956
37	3,05	2	6,5846
33	3,1	2	6,6558
28	3,15	2	6,7448
23	3,2	2	6,8338
17	3,25	2	6,9406
13	3,3	2	7,0118
9	3,35	2	7,083
6	3,4	2	7,1364
2	3,45	2	7,2076
-8	3,5	2	7,3856
-13	3,55	2	7,4746
-19	3,6	2	7,5814
-26	3,65	2	7,706
-34	3,7	2	7,8484
-39	3,75	2	7,9374
-46	3,8	2	8,062
-53	3,85	2	8,1866
-59	3,9	2	8,2934
-63	3,95	2	8,3646
-69	4	2	8,4714
-74	4,05	2	8,5604
-77	4,1	2	8,6138
-82	4,15	2	8,7028
-86	4,2	2	8,774
-90	4,25	2	8,8452
-95	4,3	2	8,9342
-99	4,35	2	9,0054
-103	4,4	2	9,0766
-107	4,45	2	9,1478
-111	4,5	2	9,219
-114	4,6	2	9,2724
-117	4,65	2	9,3258
-120	4,7	2	9,3792
-125	4,75	2	9,4682
-127	4,8	2	9,5038
-130	4,85	2	9,5572
-132	4,9	2	9,5928
-135	4,95	2	9,6462
-137	5	2	9,6818
-142	5,1	2	9,7708
-147	5,2	2	9,8598
-150	5,3	2	9,9132
-154	5,4	2	9,9844
-157	5,5	2	10,0378
-163	5,7	2	10,1446
-169	6	2	10,2514
-179	6,5	2	10,4294
-186	7	2	10,554
-192	7,5	2	10,6608
-197	8	2	10,7498
-205	9	2	10,8922
-211	10	2	10,999